



## Energy Loss of Charged Particles Traversing a Medium

In the previous lecture, when we considered the decay of charged pions in emulsion material, we saw that the energy loss of charged particles traversing a medium could be used to identify<sup>1</sup> particles and measure their properties. For example in the case of the pion decaying into a muon and a neutrino, if it is known how much energy is lost by the muon per unit length in emulsion, then one can deduce from this the kinetic energy of the muon. This can be done by measuring the muon path length from the instance that the muon was created up to the point where it stops and decays and multiply this by the energy loss per centimeter. Hence, understanding the different mechanisms under which charged particles lose energy as they traverse matter is very important in experimental particle physics.

Different particles lose energy in different ways depending if they have large or small mass, or if they interact electromagnetically, weakly or strongly with matter which of course can be used to identify them. In this lecture we will discuss about the energy loss suffered by electrons and muons as they traverse a material.

### Energy loss suffered by charged particles due to ionization

This paragraph addresses the energy loss suffered by charged particles via the process of ionization of the atoms of the material that they traverse. All charged particles lose energy this way although this is not always the dominant process of energy loss. For example the lightest of them, the electrons and positrons which have a mass of 0.511 MeV, lose energy predominately via Bremstrahlung at high energies whilst at kinetic energies of a few tens of MeVs they lose energy via ionization. Ionization is the process where charged particles interact electromagnetically with the atomic electrons in the medium and transfer energy to them via a process which results in ionizing the atoms of the medium. Calculating the energy loss using quantum theory is a fairly complicated process which is beyond the scope of this course. The correct result from the quantum mechanics calculation is given and discussed at the end. Here we will compute the energy loss classically. However, the classical calculation, whose result is not as accurate as the quantum result, does demonstrate the origin of the main features and dependencies of the quantum result.

We will start by solving the problem of calculating the energy transfer from an ionizing particle, which moves with velocity  $\vec{v}$  a distance  $d\mathbf{x}'$ , to a single stationary electron in a medium. Note that we actually compute the energy gained by the stationary electron in the medium due to the movement of the ionizing particle by  $d\mathbf{x}'$  during which time the ionizing particle is assumed to have a constant velocity  $\vec{v}$ .

<sup>1</sup> It turns out that from the other properties of the track, as we will see later, they could also tell that this was indeed a muon and not another particle.



This is a valid assumption because at the end we are only interested to compute  $dE/dx'$  (energy transfer per cm where  $dx'$  is infinitesimal) and during the time  $dt = dx'/v$  the velocity of the particle can be assumed to be constant. Eventually we will integrate over all the electrons in the medium.

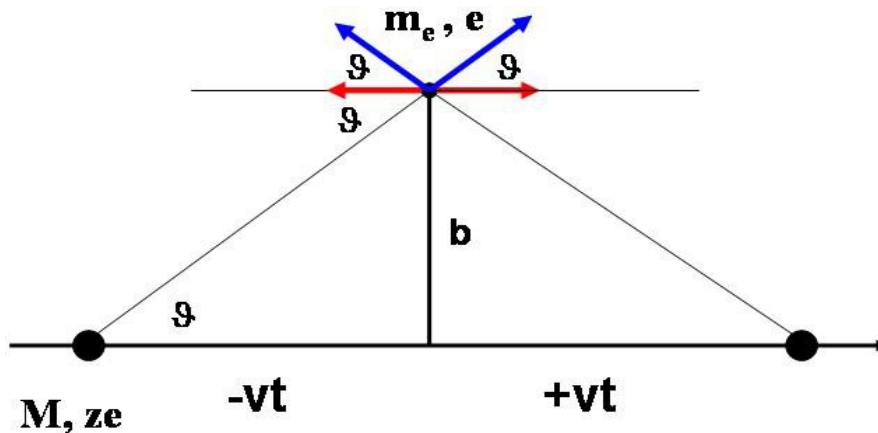


**Figure 1:** A heavy charged particle of mass  $M$ , charge  $ze$  interacts and transfers energy to a stationary electron located at distance  $b$  (impact parameter) from its path.

Consider a charged particle with charge  $ze$ , energy  $E_{LAB}$  and mass  $M$  moving along the  $z$ -axis at a distance  $b$  from a stationary electron  $e$  as shown in Fig. 1. The force on the stationary electron due to the ionizing particle in spherical and cylindrical coordinates is given by:

$$\vec{F} = \frac{ze^2}{4\pi\epsilon_0} \frac{1}{|\vec{r}(t)|^2} \hat{r} = F_\rho \hat{\rho} + F_z \hat{z}$$

Shown in Fig. 1 are the forces on the stationary electron at two different time instances. Due to the symmetry of the problem the effects due to the  $z$ -component of the force cancel out and one only needs to compute the radial force.

$$F_\rho = \frac{ze^2}{4\pi\epsilon_0} \frac{1}{|\vec{r}(t)|^2} \sin\theta = \frac{ze^2}{4\pi\epsilon_0} \frac{b}{|\vec{r}(t)|^3} = \frac{ze^2}{4\pi\epsilon_0} \frac{b}{(b^2 + (vt)^2)^{3/2}}$$

From the radial force one can calculate the radial acceleration as:

$$a_\rho = \frac{ze^2}{4\pi\epsilon_0} \frac{1}{m_e} \frac{b}{(b^2 + (vt)^2)^{3/2}}$$



Finally the radial velocity can be calculated by integrating over time:

$$V_{\rho} = \frac{ze^2}{4\pi\epsilon_0 m_e} \int_{-\infty}^{+\infty} \frac{b}{(b^2 + (vt)^2)^{3/2}} dt = \frac{ze^2}{4\pi\epsilon_0 m_e} \frac{2}{vb}$$

The energy gained by the stationary electron can be calculated using the classical formula for the kinetic energy:

$$\Delta E = \frac{1}{2} m_e V_{\rho}^2 = \frac{z^2 e^4}{8\pi^2 \epsilon_0^2 m_e v^2 b^2}$$

The integration over all the electrons in the medium is done by considering the elementary volume shown in Fig. 2. The ionizing particle is at the centre at distance  $b$  from a given electron in the medium. The elementary volume is given by:

$$dV = 2\pi b \times db \times dx'$$

and the number of electrons per unit volume is given by:  $Z \times \frac{N_A}{A} \times \rho$  where

$Z$ ,  $N_A$ ,  $A$ ,  $\rho$  are the atomic number, the Avogadro number, the mass number and the density of the medium. Hence the number of electrons is given by:

$$dn = 2\pi b db dx' \times \left( Z \times \frac{N_A}{A} \times \rho \right)$$

$$\frac{dE}{dx'} = \frac{z^2 e^4}{8\pi^2 \epsilon_0^2 m_e v^2} \times 2\pi \times Z \times \frac{N_A}{A} \times \rho \times \int_{b_{min}}^{b_{max}} \frac{b db}{b^2} \Rightarrow$$

$$\frac{dE}{dx} = \frac{z^2 e^4}{4\pi \epsilon_0^2 m_e v^2} \left( Z \frac{N_A}{A} \right) [\ln(b)]_{b_{min}}^{b_{max}}$$

where  $x = \rho x'$  and is given in units of  $g/cm^2$ .

To compute the minimum and the maximum impact parameters we use the energy formula:

$$E = \frac{1}{2} m_e V_{\rho}^2 = \frac{z^2 e^4}{8\pi^2 \epsilon_0^2 m_e v^2 b^2} \Rightarrow b_{max;min} = \frac{ze^2}{2\pi \epsilon_0 v} \frac{1}{\sqrt{2m_e} \sqrt{E_{min;max}}}$$

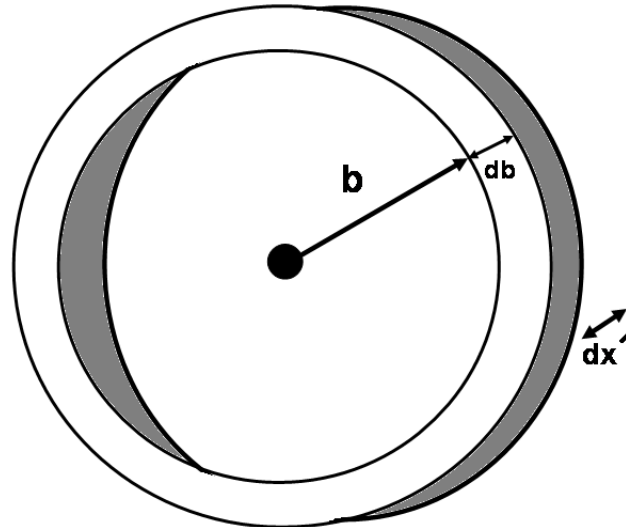


**Figure 2:** Elementary volume over which we integrate to sum the energy loss due to all electrons in the medium.

Hence,

$$\frac{dE}{dx} = \frac{z^2 e^4}{8\pi \epsilon_0^2 m_e v^2} \left( Z \frac{N_A}{A} \right) \ln\left(\frac{E_{max}}{E_{min}}\right)$$

However, the maximum energy transferred to the electron is given by:

$$E_{max} = \frac{2 m_e \beta^2 \gamma^2}{1 + \frac{2 m_e E_{LAB}}{M^2} + \frac{m_e^2}{M^2}}$$

(the proof of this formula is left as a homework). Hence, the energy loss formula is given by:

$$\frac{dE}{dx} = \frac{z^2 e^4}{8\pi \epsilon_0^2 m_e v^2} \left( Z \frac{N_A}{A} \right) \ln\left(\frac{2m_e \beta^2}{E_{min}(1-\beta^2)}\right)$$

The minimum energy  $E_{min}$  is taken to be the minimum energy required to ionize an atom of the medium, the ionization potential, and of course it depends upon the type of the medium.

Having shown the basic features of the energy loss formula we are now ready to present the exact quantum result which is the well known Bethe-Bloch formula.



**The Bethe-Bloch formula:**

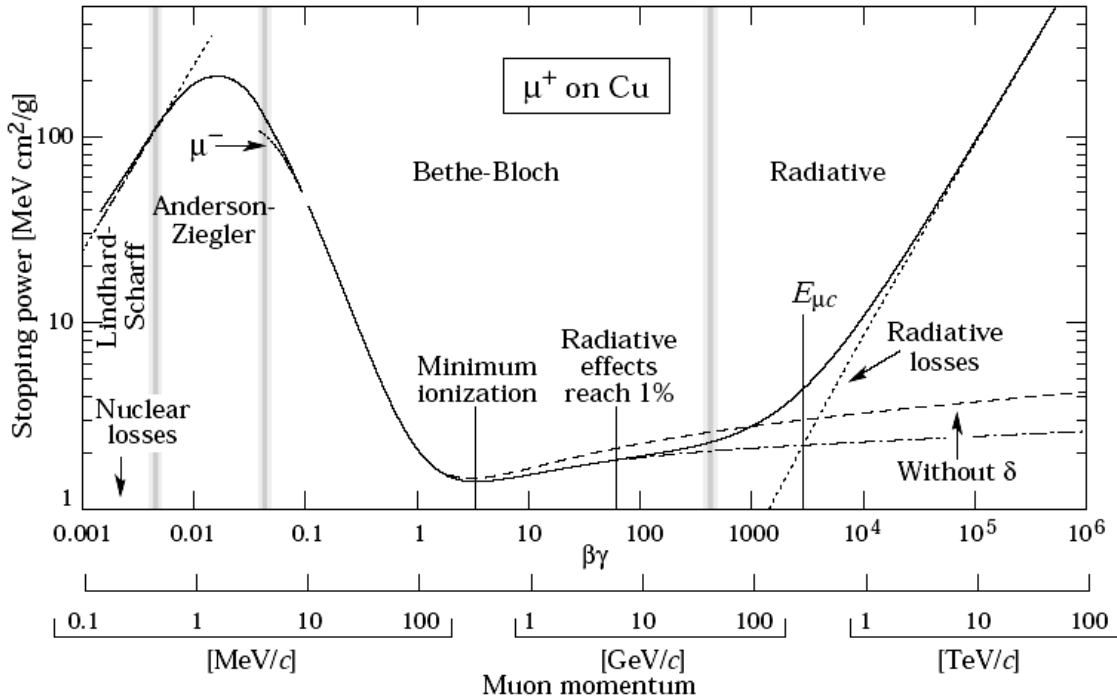


**Figure 3:** Energy loss of muons in copper. The y-axis is given in units of  $\text{MeV cm}^2/\text{g}$  so that one can multiply by the density of the given material and compute the energy loss in  $\text{MeV/cm}$ . The energy loss depends on the relativistic quantity  $\beta\gamma$  which can be converted to momentum, as it is done here for muons, if one has identified the particle and knows its mass.

The exact quantum mechanical result for the energy loss suffered by massive, charged penetrating particles is given by the Bethe-Bloch equation:

$$-\frac{dE}{dx} = K z^2 \frac{Z}{A} \frac{1}{\beta^2} \left[ \ln \frac{2m_e c^2 \beta^2 \gamma^2}{I} - \beta^2 - \frac{\delta}{2} \right] = K z^2 \frac{Z}{A} \frac{1}{\beta^2} \left[ \ln \frac{T_{max}}{I} - \beta^2 - \frac{\delta}{2} \right]$$

where:

- 1)  $\frac{K}{A} = \frac{4\pi N_A r_e^2 m_e c^2}{A} = 0.307 \text{ MeV g}^{-1} \text{ cm}^2$  if  $A = 1 \text{ g mol}^{-1}$  and  $N_A, r_e, m_e$  are the Avogadro number, the classical radius of the electron and the electron mass. The variable  $x$  is measured in  $\text{g/cm}^2$  for reasons that will become apparent later.
- 2)  $T_{max}$  is the maximum energy which can be imparted to a free electron in a single collision.



- 3)  $\beta, \gamma$  are the well known relativistic quantities,  $z$  is the charge of the incident particle and  $Z$  is the atomic number of the medium.
- 4)  $I$  is the ionisation potential usually taken to be  $I = 10 \times Z (eV)$ .
- 5) Finally  $\delta$  is the density correction term that will be discussed later.

Fig. 3 shows a plot of the Bethe-Bloch formula computed for positive muons (mass = 105.7 MeV) penetrating copper. By inspecting the Bethe-Bloch formula and Fig. 1 one can see that:

- a) The ionization energy loss does not depend upon the mass of the ionizing particle.
- b) There is only a weak dependence on the medium because  $\frac{Z}{A} \simeq 0.5$  for most materials. This can also be seen in Fig. 4 where the energy loss has been plotted for various types of materials and ionizing particles.
- c) The energy loss depends only on  $\beta$  and one needs the mass of the particle to convert it to momentum.

The Bethe-Bloch equation dictates that the energy loss increases as  $\sim \beta^{-2}$  as the particle speed decreases. This effect is also shown in Fig. 3. **This means that slow particles will be more ionizing than fast particles.** As the particle speed increases the energy loss reaches a minimum of about 1.5 – 2.0 MeV cm<sup>2</sup>/g and remains at this level for almost the entire range of muon momenta one would observe in a high energy physics experiment. Hence, **the concept of minimum ionizing particle**, which is used in high energy physics to refer to particles whose speed is in this regime and suffer similar energy losses (1.5 – 2.0 MeV cm<sup>2</sup>/g). After that it starts rising following the so called relativistic rise. However radiative effects are also important in this region.

The relativistic rise comes from the fact that the electric field of the ionizing particle in the lab frame is proportional to the relativistic gamma (coming from Lorentz transforming the electric field from the particle to the lab frame). Hence, the faster the particle is, the stronger the field becomes and therefore the particle can ionize atoms at larger distances and lose more energy. The rise of the energy loss is logarithmic as can be seen by:

$$\ln \frac{2m_e c^2 \beta^2 \gamma^2}{I} \sim \ln \frac{2m_e c^2}{I} + \ln(\beta^2 \gamma^2) \sim \ln(P/M)$$

Eventually the medium polarizes and cancels this effect. This prevents the energy loss from rising perpetually and eventually flattens at very high particle speeds. This is the origin of the density correction term,  $\delta$ , in the Bethe-Bloch equation.

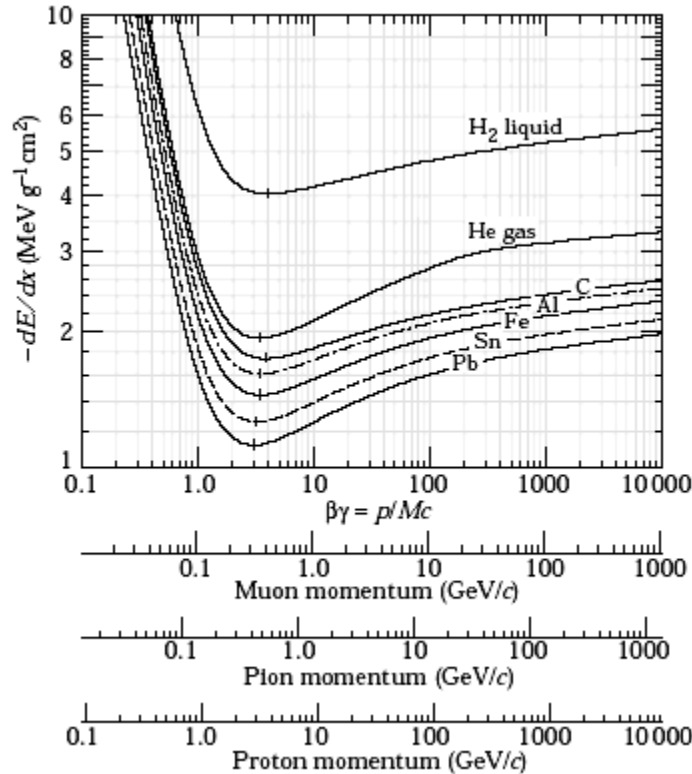


**Figure 4:** Energy loss in various types of material computed calculated for muons, pions and protons.

From the classical proof of the ionization energy loss shown earlier the reader may have realized the reasons for expressing the energy loss in  $\text{MeV cm}^2/\text{g}$ . As we said the energy loss, expressed in units of  $\text{MeV cm}^2/\text{g}$ , depends very weakly on the type of medium. However, to convert it to  $\text{MeV}/\text{cm}$  one has to take in to account how dense the material is because the Bethe-Bloch formula is given normalized to unit density. In other words a factor of density is missing which accounts for the number of electrons per unit volume for a given material. Hence in practice, although Fig. 3 refers to muons in copper, one can use it to compute energy loss in any other material by multiplying with the density of the material. Here is how one would use Fig. 3 or the Bethe-Bloch formula to calculate ionization energy loss.

**Example 1:** Consider a beam of pions each with kinetic energy equal to **80 MeV** going through a carbon block. Compute the energy loss per cm as well as the thickness of carbon required to stop them. The carbon density is  **$2.265 \text{ g/cm}^3$** . Assume that the dominant energy loss mechanism is via ionization and ignore possible effects related to the strong interaction.

**Solution:**

$$KE = E - M \Rightarrow 80 \text{ MeV} = E - 140 \text{ MeV} \Rightarrow E = 220 \text{ MeV} \Rightarrow$$

$$p = \sqrt{E^2 - M^2} = 170 \text{ MeV}/c \Rightarrow \beta\gamma = p/M = 1.21$$

One can now use the Bethe-Block formula (or Fig. 3 which is easier) to show that:

$$\frac{dE}{dx'}(\beta\gamma=1.21) \approx 2 \text{ MeV} \frac{\text{cm}^2}{\text{g}}$$

Hence,

$$\frac{dE}{dx} = 2.265 \frac{\text{g}}{\text{cm}^3} \times 2 \text{ MeV} \frac{\text{cm}^2}{\text{g}} = 4.5 \frac{\text{MeV}}{\text{cm}}$$

and with  $80 \text{ MeV} / 4.5 \text{ MeV}/\text{cm} \simeq 18 \text{ cm}$  of carbon one can stop the beam pions from going through. As we will see next this is only approximately true due to the fact the the energy loss follows the Landau distribution.





## The Landau Distribution

The ionisation energy loss is in principle a stochastic process and one should note that the Bethe-Bloch equation describes only the *average* energy loss. If one were to shoot single charged particles over and over on a target he/she will observe that the energy loss follows the Landau distribution shown in Fig. 5, where the most probable value is far lower than the average predicted by the Bethe Bloch equation.

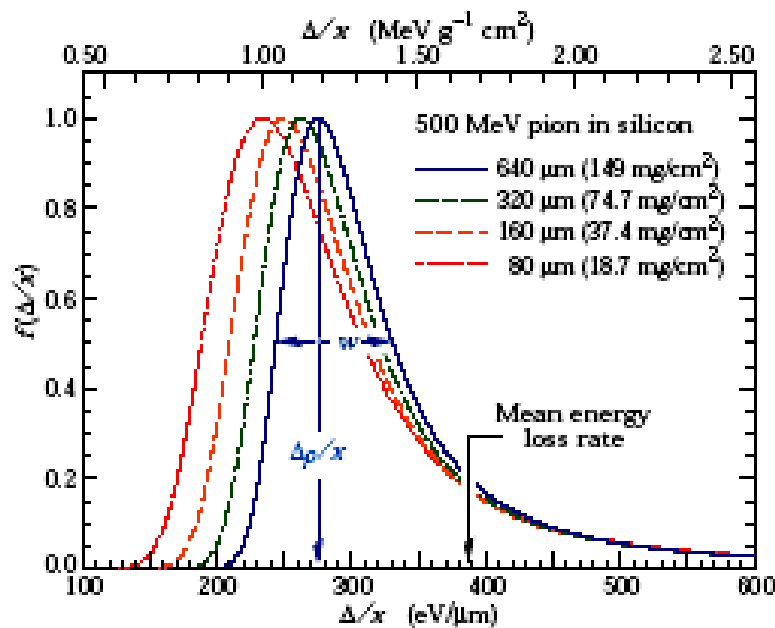


**Figure 5:** The Landau distribution which describes the energy loss for a single particle as a function of the energy loss normalized to the thickness of the material (in this case silicone).  $\Delta$  represents the energy loss and  $x$  is the thickness of the material.



### Charged Particle Identification using Energy Loss

The ionisation energy loss is often used to identify charged particles. If the particle momentum can be measured accurately then by binning the data in bins of fixed momentum we have that the ionization energy loss depends on the particle mass. Hence, by measuring  $dE/dx$  and the momentum we can identify particles relatively well as shown in Fig. 6.

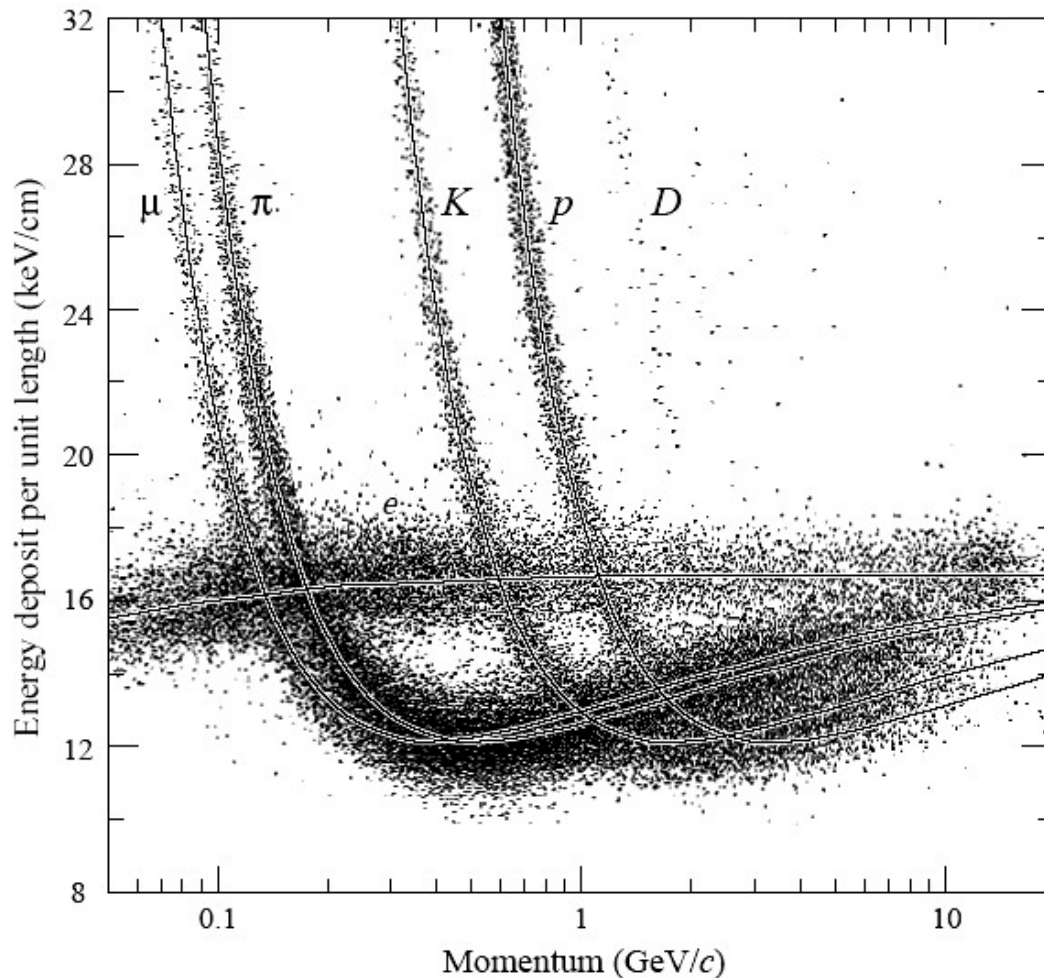


**Figure 6:** At fixed momentum the energy loss of charged particles depends upon their mass and it can be used to identify particles. The first two bands at low momentum correspond to muons and pions and the other two are for kaons and protons. A fifth band is barely seen and corresponds to D mesons which heavier than then proton. The band that is flat in momentum is the electron band.



### Multiple Coulomb Scattering

Charged particles of moderate mass traversing a medium, apart from losing energy to the electrons in the medium, interact also with the nuclei in the medium. They cannot transfer energy to them because the nuclei are much heavier than the electrons and the energy transfer, as we have seen, is inversely proportional to the target mass. However, they do ‘feel’ the Coulomb field of the nuclei and because the nuclei are a lot heavier than them, they scatter transversely in the field of the nuclei. The elementary process for one such a scatter is well understood since more than a hundred years ago and it is described by the Rutherford formula. However, one has to take in to account that a charged particle moving in a medium will undergo a large number of such scatters in a process which is stochastic in nature and it is called *Multiple Coulomb Scattering*.

From the experimental physics point of view one needs to be able to compute how much a charged particle beam is going to diffuse when it goes through a medium. Clearly, due to this effect, one expects that even a pencil beam of infinitely small cross section passing through a medium of some thickness, will diffuse. At the exit point its spacial distribution will be Gaussian due to the stochastic nature of the scatters but it will have non-Gaussian tails due to the Rutherford formula as shown in Fig. 7.

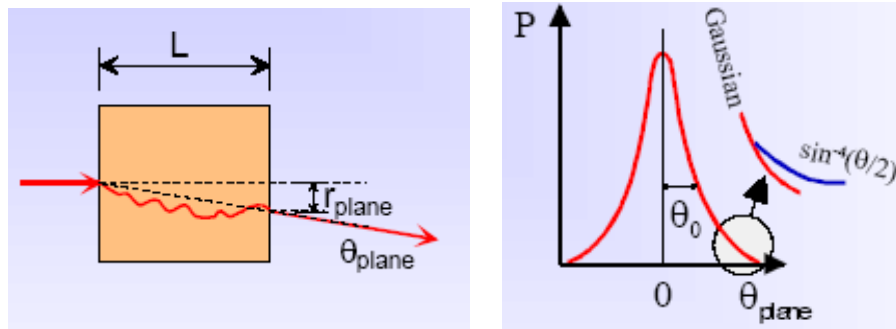


**Figure 7:** A particle beam passing a material of length  $L$  undergoes multiple Coulomb scattering and at the exit point the particles of the beam follow a Gaussian distribution with non-Gaussian tails.

It turns out that the RMS of the angular distribution in space is given by the formula:

$$(\theta_{RMS})^2 = \left( \frac{z E_s}{p \beta} \right)^2 \times \frac{dL}{X_0}$$

where  $z$  is the charged particle charge number,  $E_s = 21 \text{ MeV}$ ,  $p, \beta$  are the momentum and the relativistic velocity of the particle,  $dL$  is the elementary length of the material that the particle went through and caused the deflection and  $X_0$  is the **radiation length in cm** which is a constant that depends upon the material and will be discussed later.



If one is interested to compute the deflection on the trajectory plane as shown in Fig. 7 an extra factor of  $\sqrt{2}$  need to be introduced:

$$(\theta_{RMS})_{PLANE}^2 = \left( \frac{z E_s}{p \beta \sqrt{2}} \right)^2 \times \frac{dL}{X_0}$$

### Energy Loss by Electrons

The dominant process that the electrons lose energy when they pass through a material and have kinetic energy above some tens of MeV is shown in Fig. 8. and it is called Bremsstrahlung radiation. The key idea to this diagram is that an electron in absolute vacuum cannot just radiate a photon. To do this it must exchange a soft photon with a heavier nucleus in its neighborhood<sup>2</sup>.

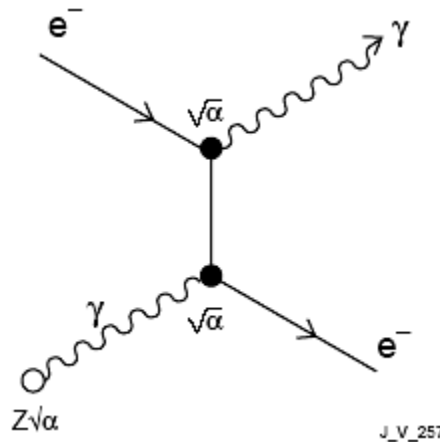


**Figure 8:** The Bremsstrahlung process.

Lets try to guess the cross section of this process: From the strength of the electromagnetic interaction and basic Feynman digram rules we expect that amplitude for this process will be:

$$A \sim Z e^3 \sim Z \alpha_{QED}^{3/2}$$

and the cross section will be:

$$\sigma \sim |A|^2 \sim Z^2 e^6 \sim Z^2 \alpha_{QED}^3$$

<sup>2</sup> To show this go to the rest frame of the incident electron and compute the kinematics of  $e \rightarrow e \gamma$ .



However, this has the wrong units since it is obviously a number. The only other variable involved in this problem is the electron mass and to get the correct units for cross section (length square) one needs to divide by the electron mass square which has units of one over length.

$$\sigma \sim |A|^2 \sim \frac{Z^2 e^6}{m_e^2} \sim \frac{Z^2 \alpha_{QED}^3}{m_e^2}$$

Of course this is units of  $\text{GeV}^{-2}$  which in our system of units is the unit of length square. If one wants to convert this to square meters, he must multiply or divide by factors of  $\hbar, c$  to get the correct units. It turns out that the formula then becomes:

$$\sigma \sim \frac{Z^2 \alpha_{QED}^3}{m_e^2 c^4} \times (\hbar c)^2$$

Now it should be obvious why the electrons behave radically different than the muons: The radiation rate is inversely proportional to the square of the mass. The muons radiate also but  $(m_e/m_\mu)^2 \sim (1/200)^2$  less than electrons. Hence, in the energy range of today's experiments, the effect is negligible and the muons can only lose energy via the Bethe-Bloch process. In the case of the much lighter electrons the dominant process is indeed Bremsstrahlung, which sometimes is called Bethe-Heitler process, except for energies below a the critical energy that we will be discussing shortly.

Lets proceed now to compute the  $dE/dx$  for electrons due to the Bremsstrahlung process:

$$\frac{d\sigma}{dE} \sim \frac{Z^2 \alpha_{QED}^3}{m_e^2 c^4} \times \frac{(\hbar c)^2}{E} \Rightarrow$$

where  $E$  is the energy transferred. The total energy transferred over an interval  $dx$  is then computed as follows.

$$-\frac{dE}{dx} \sim n \int_{E_{min}}^{E_{max}} E \times \frac{Z^2 \alpha_{QED}^3}{m_e^2 c^4} \times \frac{(\hbar c)^2}{E} dE = n \frac{Z^2 \alpha_{QED}^3}{m_e^2 c^4} (\hbar c)^2 (E_{max} - E_{min})$$

where  $n$  is the number of nuclei per cubic centimeter and  $E_{max}, E_{min}$  are the maximum and the minimum energy transfer. The later can be taken to be almost zero. An extra factor of  $4 \ln(183/Z^{1/3})$  is needed to account for integrating over the range of possible impact parameters and the result then reads:



$$\frac{dE}{dx} = -4n \frac{Z^2 \alpha_{QED}^3 (\hbar c)^2 \ln\left(\frac{183}{Z^{1/3}}\right) E}{m_e^2 c^4} \quad (E = E_{max})$$

where the relationship

$$\frac{1}{X_0} = 4n \frac{Z^2 \alpha_{QED}^3 (\hbar c)^2 \ln\left(\frac{183}{Z^{1/3}}\right)}{m_e^2 c^4}$$

defines the **radiation length**. It is worth noting here the radiation length of a given material is inversely proportional to the square of the atomic number of the material. This means that if the goal is to absorb rapidly an electromagnetic cascade one needs to use a high-Z material such as iron, tungsten, lead, uranium or another such material.

In conclusion,

$$\frac{dE}{dx} = -\frac{E}{X_0} \Rightarrow E(x) = E_0 e^{-\frac{x}{X_0}}$$

In practical terms this relationship dictates that after one radiation length the electron has 1/e of its energy left. As shown here the radiation length has units of length. However, often it is given in units of g/cm<sup>2</sup> and one has to divide by the density of the material to convert it to centimeters<sup>3</sup>.

One would then ask when does the electron lose energy via the Bremstrahlung process and when via the Bethe-Bloch process. As one may guess the faster the electron is the more likely is to radiate photons as it slows down while entering a space filled in with material. Eventually its energy will become significantly lower. At low energies the ionization (Bethe-Bloch) process dominates. This is shown in Fig. 9 which describes electron and proton energy loss in copper. For electrons below 10 MeV the Bethe-Bloch process dominates and above that the Bremstrahlung process, which rises linearly with energy, becomes dominant.

<sup>3</sup> [https://pdg.lbl.gov/2022/html/computer\\_read.html](https://pdg.lbl.gov/2022/html/computer_read.html)

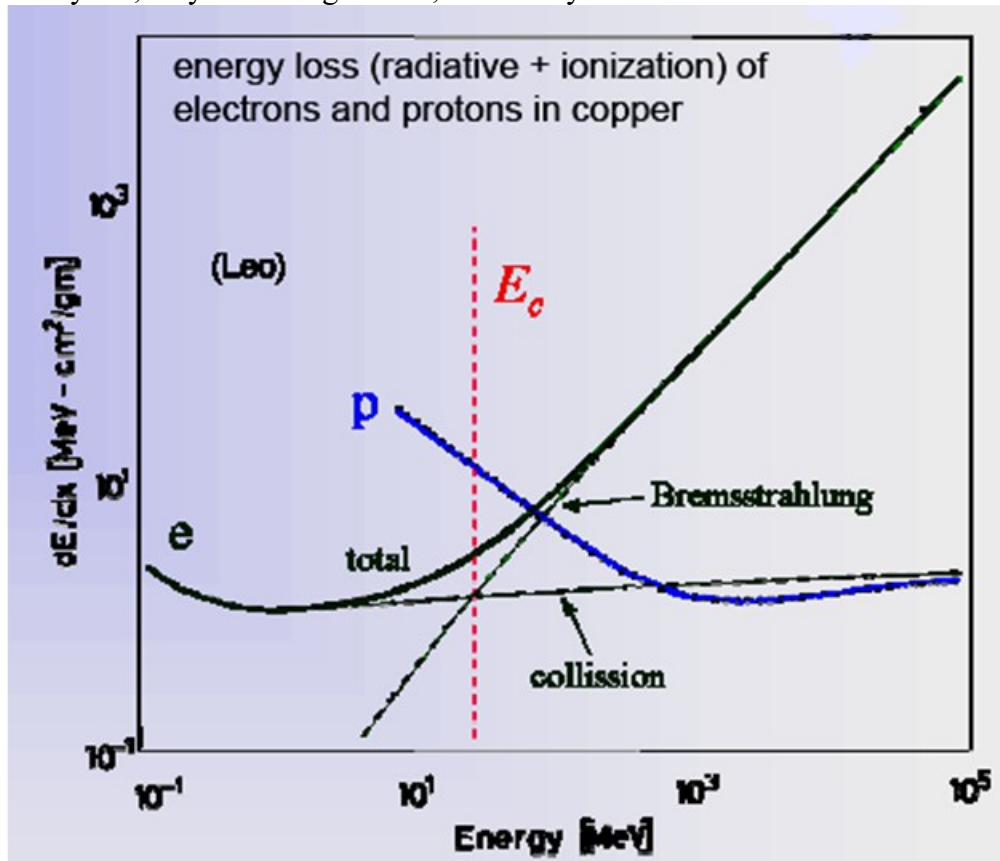


Figure 9: Contributions to the energy loss by electrons as a function of energy in MeV.

The energy where the Bethe-Bloch contribution is equal to the Bremsstrahlung contribution is called **critical energy** and depends inversely proportional to the atomic number of the material involved. The critical energy is given by:

$$E_c \approx \frac{560 \text{ MeV}}{Z}$$

Obviously this is an approximate formula and in practice it is different for gases, liquids and solids. One finds in the literature also the following different formulas for solids-liquids and gasses.

$$(E_c)_{\text{Solid/Liquid}} \approx \frac{610 \text{ MeV}}{Z+1.24} \quad ; \quad (E_c)_{\text{Gas}} \approx \frac{710 \text{ MeV}}{Z+1.24}$$

These are clearly approximations derived from data.



## Electromagnetic Cascades (Showers)

Lets try to get an idea of what happens when an electron beam hits a target. From what we have learned so far the electron will emit a Bremstrahlung photon again and again via a process that the electron loses energy until its kinetic energy decreases down to the critical energy where the radiation process becomes negligible and the energy loss due to ionization dominates. The photons from the electron if they are energetic enough will create electron-positron pairs which in turn will radiate again. If they are not energetic enough they will lose energy via the Compton or the Photoelectric effects. The entire collection of these photons, electrons and positrons is called *electromagnetic shower* or *electromagnetic cascade*.

So lets create a simple model to describe this process. Lets assume that for every radiation length that the particles propagate in the material an electron-positron pair is created if the parent particle is a photon or an electron-photon pair is created if the parent particle is an electron. The process is shown in Fig. 10 and starts with a photon but it could have equally well have started with an electron emitting a photon. The student who thinks that this model is simplistic should look to Fig. 11 and convince herself/himself that these things actually happen in the way we have hypothesized. Clearly, according to our model, the number of particles created rises as:

$$N(t) = 2^t$$

where  $t$  is the number of radiation lengths in the material. The process goes on until all the particles have reached the critical energy. From this point on the electrons in the shower lose energy by ionizing the material around them and get absorbed. Photons keep pair-creating until their energy is below 1 MeV after which point they lose energy only via the Compton and the Photoelectric effects. Obviously this is an approximation but a good one.

Next we can calculate at which point we will have reached the maximum number of particles. The average energy of each particle at a depth of  $t$ -radiation lengths is:

$$E(t) = \frac{E_0}{2^t}$$

The maximum number of particles is reached when:

$$E_c = \frac{E_0}{2^{t_{max}}} \Rightarrow \ln\left(\frac{E_c}{E_0}\right) = -\ln 2 \cdot t_{max} \Rightarrow t_{max} = \frac{1}{\ln 2} \ln\left(\frac{E_0}{E_c}\right)$$



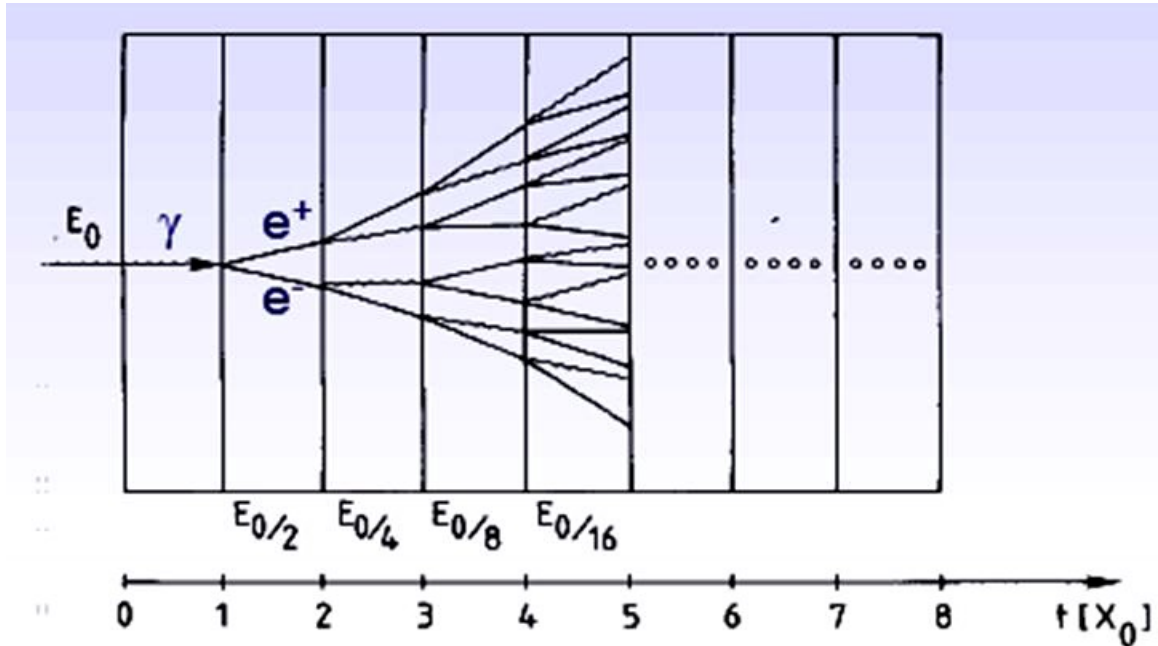


**Figure 10:** A model of the electromagnetic cascade where one assumes that one electron-positron or an electron-photon pair will be created for every radiation length in the material in a process that subdivides the energy of the original particle until the particles reach the critical energy for the specific material.

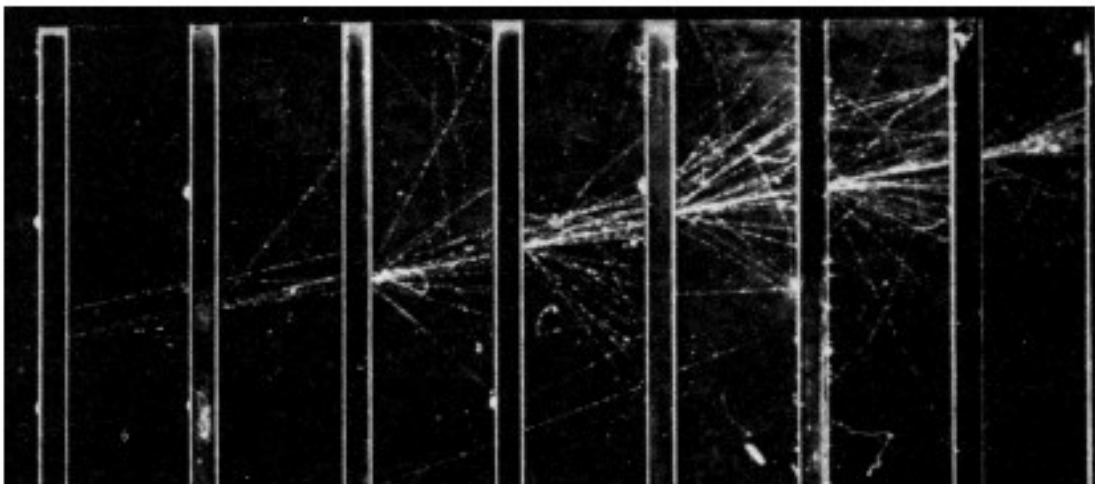


**Figure 11:** An actual picture of an electromagnetic cascade in a cloud chamber instrumented with metal plates to force the electron to lose energy.



Another approximation of this formula is given by:

$$t_{max} = \ln\left(\frac{E_0}{E_c}\right) + 0.5 \quad (X_0) \text{ which is valid for photons.}$$

and

$$t_{max} = \ln\left(\frac{E_0}{E_c}\right) - 0.5 \quad (X_0) \text{ which is valid for electrons.}$$

As seen here electromagnetic showers originating from electrons reach their maximum about one radiation length deeper than those originating from photons. This is expected because the photons need about a radiation length to produce an electron positron pair. Note that the depth at the shower maximum is given in units of radiation lengths.

The reader should compare these formulas with the data from Fig.12 to convince himself/herself that they work. **All these formulas indicate that that the electromagnetic shower depth grows logarithmically with the shower energy.** This is very fortunate because it means that the size of the detectors that measure energy also grows logarithmically with energy.

Next we can try to derive roughly the number of particles created.

$$N_{TOTAL} = \sum_0^{t_{max}} 2^t = 2^{t_{max}+1} - 1 \simeq 2^{t_{max}+1} = 2 \cdot 2^{t_{max}}$$

and substituting for  $t_{max}$  we have:

$$N_{TOTAL} \simeq 2 \frac{E_0}{E_c}$$

**Hence, the number of particles in a shower grows linearly with energy.** This fact has been exploited for making measurements of the shower energy. Alternatively dividing the incident electron or photon energy by the critical energy gives an estimate of the number of particles created. However, if one wants to contain the electromagnetic shower will need to place material of depth larger than  $t_{max}$ . As seen from Fig. 12, for a 95% containment one would have to add approximately 10 radiation lengths of material to allow all the particles to lose their energy via ionization and get absorbed. The equation which gives the 95% containment of an electromagnetic shower is:



$$t_{95\%} \simeq t_{max} + 0.08 Z + 9.6 \quad (\text{in units of radiation lengths})$$

Finally the transverse size of an electromagnetic shower is characterized by the **Moliere radius** which is given by:

$$R_M = \frac{21 \text{ MeV}}{E_c} X_0 \quad \text{or}$$

$$R_M = 7 \frac{A}{Z} \text{ g cm}^{-2} \quad (\text{need to divide by density})$$

For 95% transverse containment one would use

$$R_{95\%} = 14 \frac{A}{Z} \text{ g cm}^{-2}$$

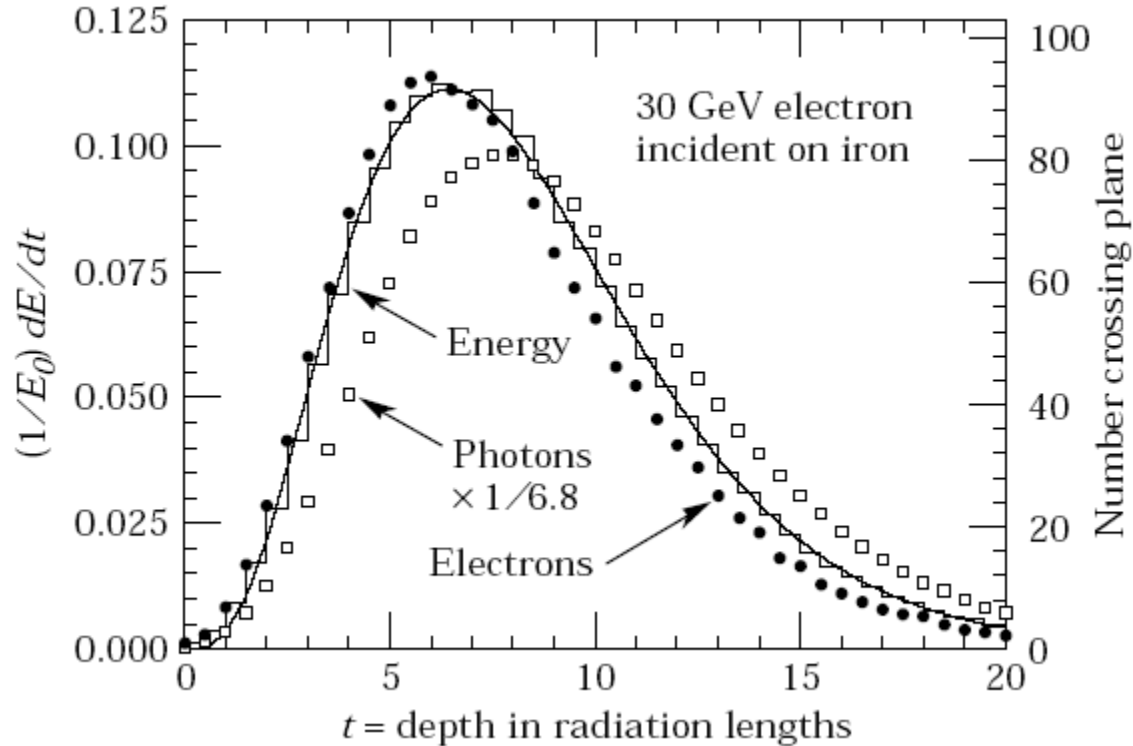


**Figure 12:** The normalized differential distribution of energy deposition in iron from 30 GeV Electrons.



**Calorimeters:** These are instruments that measure the energy of an electromagnetic shower by essentially measuring the total number of particles in the shower. Given that the number of particles produced depends linearly on the energy deposited one needs only a few calibration measurements using test beams of well known energy to calibrate a calorimeter. There are uniform and sampling calorimeters.

Uniform calorimeters are instruments made typically of active materials with short radiation length which absorb the entire electromagnetic shower and convert the cascade energy deposited to light which can be measured using light sensitive devices such as photomultipliers. Uniform calorimeters are active throughout their volume. As stated before, ultimately all shower particles, as they lose energy, reach the critical energy,  $E_c$ , where they lose energy via ionization at a fixed rate described by  $(dE/dx)$ . The amount of energy released in the form of light is equal to the number of particles produced multiplied by the minimum ionizing energy deposition of each particle. Hence, the amount of light produced and the number of particles are proportional to the energy deposited on the calorimeter.

**Example:** Consider a uniform calorimeter with  $E_c = 10 \text{ MeV}$ . Estimate the number of particles produced in this calorimeter when a photon of energy  $E_\gamma = 20 \text{ GeV}$  enters the calorimeter.

**Solution:** Based on the previous discussion the number of particles is given by

$$N_{tot} \sim \frac{E_\gamma}{E_c} = \frac{20 \text{ GeV}}{10 \text{ MeV}} = 2000$$

A sampling calorimeter does not 'see' all the energy of the electromagnetic shower but only a fraction of it. It is typically constructed by plates of absorber of thickness,  $d$ , with layers of active material in placed in between. Sampling calorimeters are cheaper to construct but they can never compete in energy resolution with the uniform calorimeters simply because a sampling calorimeter does not measure the entire electromagnetic cascade. An example of a sampling calorimeter is shown in Fig. 13.

The energy resolution of a calorimeter is given by

$$\frac{\Delta E}{E} = A \otimes \frac{B}{\sqrt{E}} \otimes \frac{C}{E}$$

where the symbol  $\otimes$  indicates addition in quadrature.



The constant term,  $A$ , is due to uncertainties in the uniformity and inter-calibration of the the various calorimeter elements. The  $B/\sqrt{E}$  term is called the stochastic term and originates from fluctuations of the particles in electromagnetic shower. Since the incident energy is proportional to the number of particles produced the stochastic term of the resolution can be estimated using Poisson statistics:

$$\frac{\Delta E}{E} \sim \frac{\sqrt{N_{TOT}}}{N_{TOT}} = \frac{1}{\sqrt{N_{TOT}}} \sim \frac{1}{\sqrt{E}}$$

For example the intrinsic resolution of the calorimeter of the previous example for photon energy equal to 20 GeV would be

$$\frac{\Delta E}{E} \sim \frac{1}{\sqrt{E}} = \frac{1}{\sqrt{2000}} \approx 2\%$$

The term  $C/E$  has its origin in noise. The constant, stochastic and noise uncertainty contributions are independent errors and to compute the total error one will have to add them in quadrature.

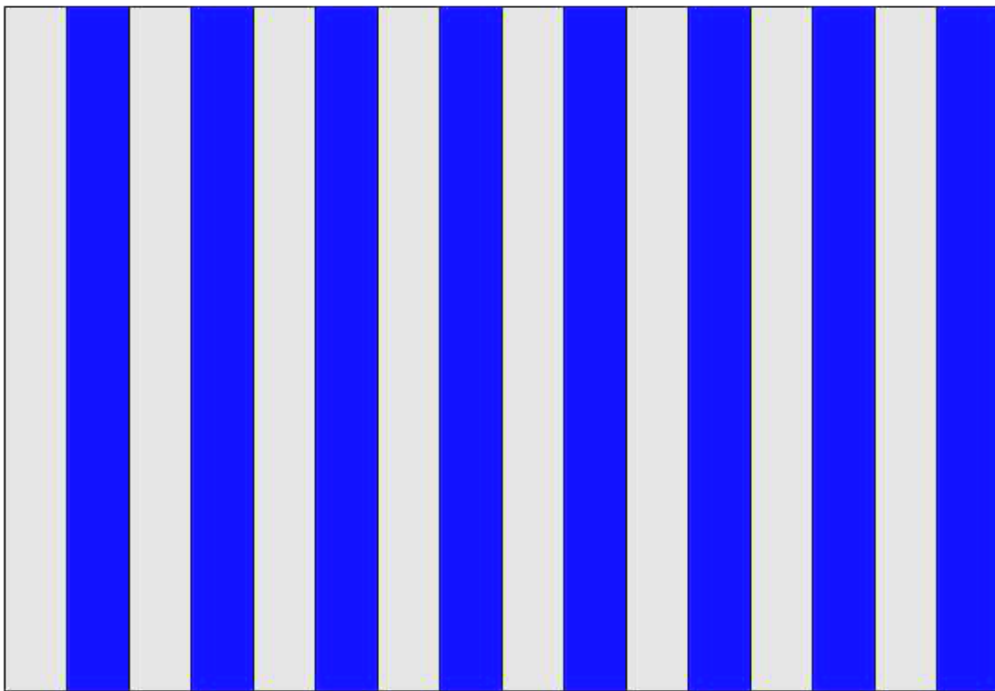


**Figure 13:** A sampling calorimeter with absorber plates of thickness,  $d$ , shown in gray and active material placed in between them.



The stochastic term of the calorimeter resolution can be computed roughly from

$$\frac{\Delta E}{E} \sim \frac{\sqrt{F_{Fano}} \sqrt{W}}{\sqrt{E}}$$

where  $F_{Fano}$  is a factor which accounts for the fact that the overall energy does not fluctuate (Fano factor) since the energy of the beam that impinges in the calorimeter is fixed and  $W \sim E_c$  is the energy typical to a single interaction. Note that  $E/W$  is proportional to the total number of particles created. The assumption here is that at the shower maximum all particles have approximately and energy equal to  $E_c$  which the subsequently lose via ionization.

The a more accurate expression for the stochastic term of a sampling calorimeter is given by

$$\frac{\Delta E}{E} = \sqrt{\frac{E_c d}{F f E_0 X_0}}$$

where  $E_0, E_c, X_0$  are the incident particle energy, the critical energy of the absorber, and the radiation length of the absorber in cm. The quantity  $f$  is the sampling fraction of the calorimeter (the percentage of energy deposited on the active material) and  $F$  is a correction factor which takes in to account that some particle tracks are lost due to the energy cutoff of the calorimeter (most calorimeters are insensitive to particles of energy below some MeV). As the reader realizes the quantity  $E_0/(E_c d/X_0)$  is simply the number of particles of the shower.

As active material in uniform calorimeters one wants to use a material that produces enough light from the electromagnetic cascade and also has a short radiation length so it absorbs the cascade in a way that the calorimeter size remains reasonable. For example the CMS collaboration at CERN has used crystals of  $\text{PbWO}_4$  in the design of its electromagnetic calorimeter.

In sampling calorimeters liquid or plastic scintillator, liquid Argon or silicon have been used as active materials.

In general the performance of the calorimeter is determined by the radiation length  $X_0$ , the critical energy  $E_c$ , and the attenuation length  $\lambda_{att}$  which determines how the shower decreases after it has reached its maximum. In addition to these for sampling calorimeters the sampling fraction is key to their performance.



## The Cloud Chamber

A number of important measurements in the early years of particle physics were done using an instrument called the Cloud Chamber. By today's standards the Cloud Chamber is a very crude instrument and can easily be constructed in an undergraduate lab with a budget of the order of 50-100 Euro. However, the discovery of the positron, the muon, the strange particles and our early knowledge on the nature of cosmic rays have their origins to this device. The cloud chamber was developed by C.T.R. Wilson (Cambridge) in 1896 who got the Nobel price for his invention in 1927.

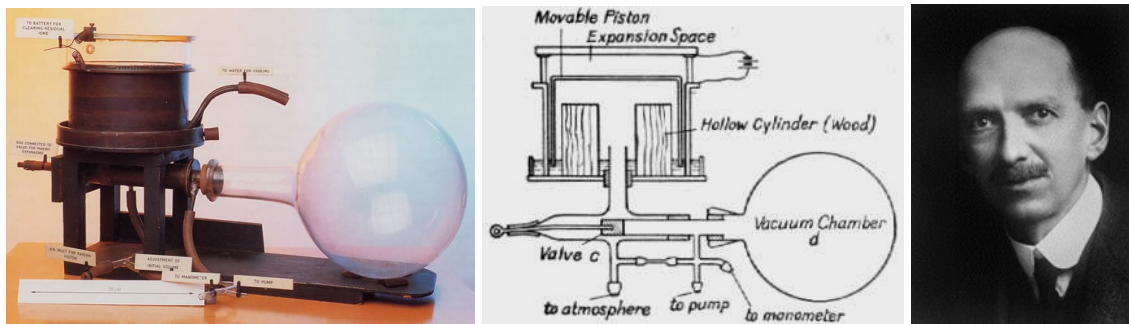


**Figure 14:** A picture of the expansion cloud chamber (Left). The cloud chamber is at the top left of the device. The glass vacuum chamber is shown to the right. The black metal cylinder contains a piston which was driven by the vacuum using valves. The detailed design of the instrument is shown in the picture at the center. A picture of the inventor of this device, C.T.R. Wilson, is shown to the right.

A typical example of an early Cloud Chamber is shown in Fig 14. This is an expansion type Cloud Chamber and works as follows: The chamber at the top left is filled with a vapor which is usually alcohol or a mixture of alcohol and water. The vacuum chamber to the right is controlled by a valve and is used to 'suck-down' a piston. The resulting expansion of the vapor in the chamber cools it and thus creates a supersaturated atmosphere. This means that the vapor temperature is lower than the normal temperature that the vapor exists and will immediately condensate under certain conditions. However, supersaturated vapor will not condensate unless if it is seeded. When a charged particle goes through the chamber it ionizes the medium. The positive ions provide such a condensation seed and condensation starts along the charged particle path. Hence, charged particle paths can be observed by the small droplets they leave behind. In the early days of the Cloud Chamber work the chamber would be illuminated from one side and pictures would be made from the other side. If an interaction occurred when the picture was made, it was recorded. As the reader may guess this not a very efficient way of doing this and a method to *trigger* the camera to record pictures only when an interaction had occurred was later introduced by P.M.S. Blackett who also got a Nobel price for his contributions to research using Cloud Chambers.



Often the Cloud Chamber was put in a magnetic field which was used to bend the particle trajectories and measure their momentum using the formula:

$$R(m) = \frac{p(\text{GeV})}{0.3 B(\text{Tesla})}$$

where **R** is the radius in meters **p** the momentum in GeV and **B** the magnetic field in Tesla.

It was also a usual practice to insert a metal sheet in to the chamber. This forced electrons or positrons traversing the sheet to lose a substantial amount of energy over a short distance. As one expects intuitively the energy loss per centimeter in a metal must be far larger than that in a gas (the radiation length decreases as  $\sim Z^{-2}$ ). This meant that the electrons or positrons exiting the metal would bend more in the magnetic field than before entering. Hence, one could tell their direction from which they deduced the sign of their charge. In addition the energy loss of different particles as they traversed the metal sheet could be measured. These measurements were used to identify the particles.

Figures 15 and 16 show typical pictures taken by Cloud Chambers. Figure 15 shows several electrons and positrons. The positrons and electrons bend in opposite directions in the magnetic field of the chamber due to their opposite charges. In addition to the 6 high momentum tracks one can clearly see 2 tracks which curl more in the magnetic field of the chamber because they have considerably less momentum. These two tracks have been identified as those of an electron and a positron which were pair-produced by a photon radiated of one of the primary electrons. Hence, their momentum is smaller than the primary electron.

Figure 16 shows a Cloud Chamber with a piece of an absorber sheet placed in the chamber. Particles colliding with it produce showers of new particles which can be seen at the other side of the absorber sheet. One of the particles produced is a neutral kaon decaying to two charged pions. This was the first evidence of a new category of particles, which were called strange particles, because although they could be produced copiously, which was an indication of being produced by the strong interaction, they would decay relatively slowly which was an indication that they decay via the weak interaction.



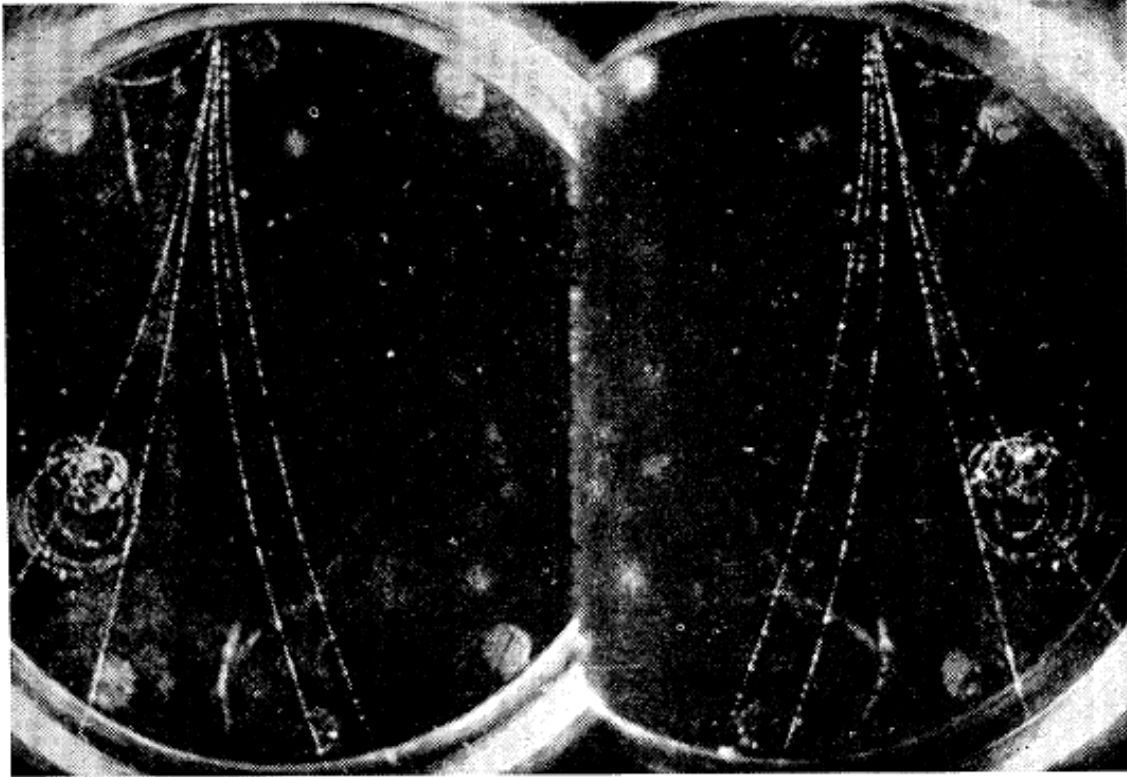


**Figure 15:** Two pictures of a Cloud Chamber event. The picture to the left is taken from the top side of the chamber and shows 3 electrons (left side) and 3 positrons (right side). The picture to the right shows the same event shown from the bottom of the chamber. The slow particles which curl more in the magnetic field are the result of a photon radiated from the electron which subsequently splits in to an electron-positron pair.



**Figure 16:** A famous picture from a Cloud Chamber. The metal sheet can be clearly seen in the middle of the chamber. Also clear is that some particles lose energy rapidly and their paths degenerate to curly tracks where other particles don't and follow somewhat straighter trajectories bent slightly only due to the magnetic field. This picture is famous because at the lower right side it shows for first time the decay of a neutral strange particle into two charged pions which was measured by Rochester and Butler in 1947.



### The Discovery of the Muon (1937)

In 1937 S.H. Neddermeyer and C.D. Anderson<sup>4</sup> at Caltech measured the energy loss of cosmic ray particles as they passed through an 1 cm plate of platinum placed in a Cloud Chamber. The Cloud Chamber was placed in a uniform magnetic field so that the curvature of the particle trajectories could be measured before entering the platinum and after exiting the platinum. Hence, they could compute the energy loss suffered by particles. Obviously what was actually measured was the particle momenta from which one could infer the energies of the particles if he/she assumed the mass. This was not very hard those days since they knew only for types of particles, the proton, the neutron, the electron and the positron which had recently been discovered and would be the subject of discussion later on in the course. What Neddermeyer and Anderson found is summarized in Figure 17.

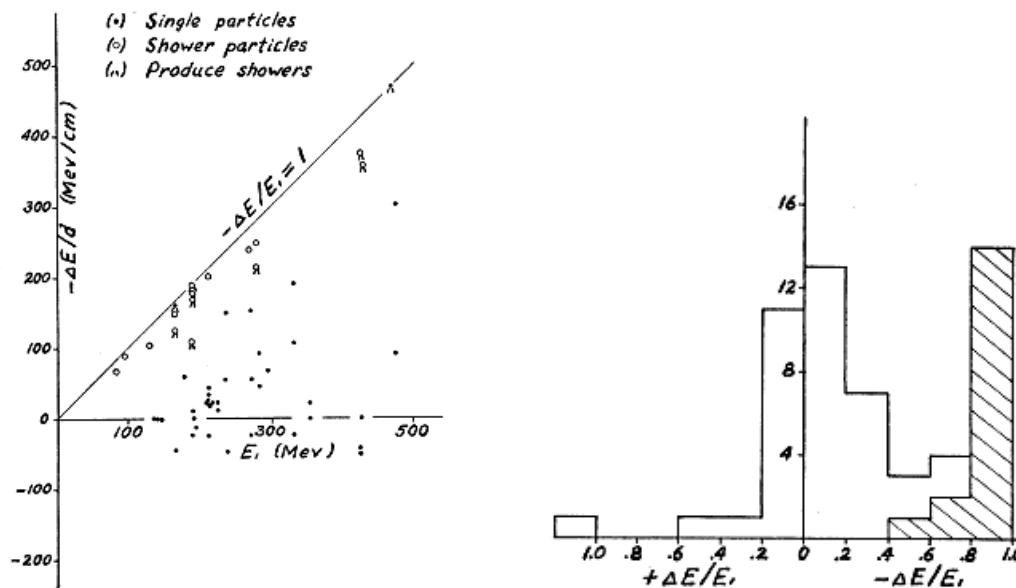


**Figure 17:** The energy loss of particles plotted versus the particle initial energy (left). The histogram to the right shows the number of events versus the percent energy loss. The events shown at the negative side of the histogram are due to experimental resolution but also due to tracks which move upwards whereas they have been accounted as downwards going tracks.

<sup>4</sup> S. H. Neddermeyer, C. D. Anderson, Phys. Rev. 51, p884, (1937)



Their results demonstrate that there were two categories of particles:

- I. Particles that lost a significant fraction of their energy in the platinum. The energy they lost was proportional to their initial energy in agreement with the Bethe Heitler theory ( $dE/dx = (-E/X_0)$ ). Hence, they are concentrated close to the straight line of Fig. 16 (left) and are also shown as the shaded histogram in Fig. 16 (right) concentrated between 0.8 and 1.0 (significant part of their energy lost). Based on these, these particles were identified to be electrons and positrons.
- II. Penetrating particles which lose a small fraction of their energy in platinum. These are shown clearly as a band close to the x-axis in Fig. 16 (left) and in the histogram of Fig. 16 (right) where they are concentrated below 0.2 (energy loss less than 20% of the initial energy).

The penetrating particles of category II were new and unexpected and of course the big question was what kind of particles they were. To figure this one out, one has to know how do charged particles lose energy due to ionisation in the medium that they traverse. They were not protons because the momentum accessible to this experiment was below 500 MeV/c and protons of this kinetic energy would be highly ionizing since they would be very slow. The highest momentum track had a momentum of :

$$p = 0.3 \cdot B \cdot R = 0.3 \times 4.5 \times 10^5 \text{ Gauss} \cdot \text{cm} = 135 \text{ MeV}/c$$

Hence, if they were protons they would have had :

$$\beta\gamma = (135 \text{ MeV})/938 \text{ MeV} = 0.14$$

which would place them right in the low  $\beta\gamma$  region of the Bethe-Bloch formula where the energy loss rises with decreasing particle velocity and is approximately  $10 \text{ MeV cm}^2/\text{g}$ . This would have been manifested by thick tracks with the high density of droplets which was of course not observed. A proton track at this speed would have had a track that had 25 times larger droplet density than that from an electron of the same momentum.

They were not electrons either. Electrons of momentum  $135 \text{ MeV}/c$  are fast and have:

$$\beta\gamma = (135 \text{ MeV})/0.511 \text{ MeV} = 264.2$$

Although the energy they would lose via ionization is small  $\sim 2.0 \text{ MeV cm}^2/\text{g}$ , they should have lost a significant fraction of their energy via Bremstrahlung,  $dE/dx = (-E/X_0)$  and the energy loss should have been proportional to their original energy, which according to the data shown in Fig. 17 was not the case for the category II of the penetrating particles.



Hence, Anderson and Neddermeyer claimed discovery of new particles which were neither electrons (or positrons) nor protons (they only particles known at the time). Stevenson and Street<sup>5</sup> followed up with their experiment shortly after them investigating the nature of these penetrating particles.

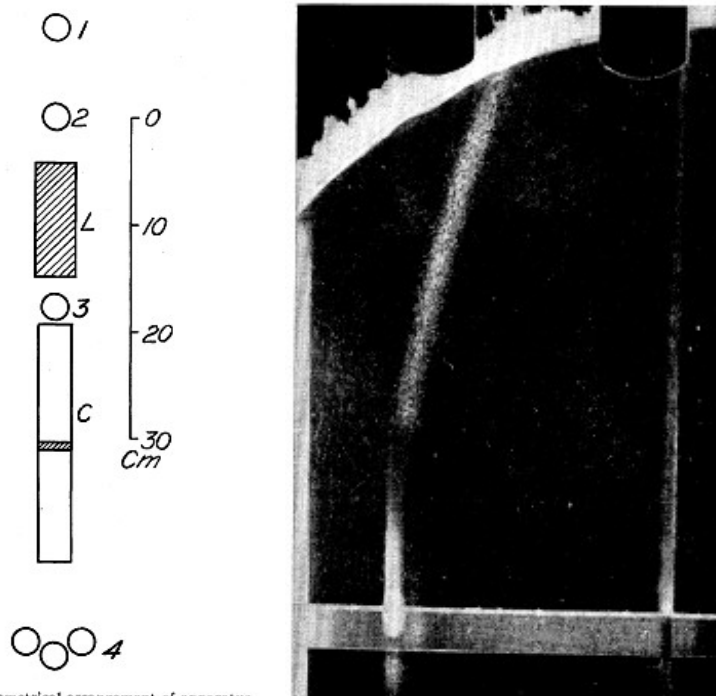


FIG. 1. Geometrical arrangement of apparatus.

**Figure 18:** The apparatus of Stevenson and Street (left) selected particles which stopped in the cloud chamber, C, using a trigger which fired when Geiger counters 1,2,3 had fired and counters 4 had not fired. Hence, it selected particles whose energy was a little larger than the energy loss suffered in the lead block L. One of these events is shown in the picture to the right.

Stevenson and Street used the cloud chamber apparatus of Fig. 18 (left) placed in a magnetic field. The technique they used to *trigger* the camera of the cloud chamber had been pioneered earlier by Blackett (who got the Nobel for this technique among other things he did). They used Geiger counters which fired when a charged particle went through. The signals from the Geiger counters triggered the camera of the cloud chamber to take a picture of the cloud chamber. This way pictures were taken only when particles went through and not at random.

Stevenson and Street designed their apparatus to select slow particles which stopped in the cloud chamber. This way they could clearly measure well both the track momentum (they bend a lot) as well as the track ionization (  $\sim 1/\beta^2$  ) by measuring the droplet

<sup>5</sup> J. C. Street, E. C. Stevenson, Phys. Rev. 52, p1003, (1937).



density of the tracks. The trigger condition to record a picture were that Geiger counters 1, 2, 3 had fired but Geiger 4 had not fired ( $1 \cdot 2 \cdot 3 \cdot \bar{4}$ ). This way the particle whose picture was taken must have stopped in the chamber. However, the average kinetic energy of cosmic ray muons is about 1 GeV. Muons of such energy would have penetrated the cloud chamber and would have exited firing Geiger 4 because the energy loss due to ionization in the cloud chamber is far less than 1 GeV. To slow them down a lead block was placed between counters 2 and 3. We assume that the thickness of the lead block was optimized to maximize the muons stopping in the chamber.

Furhtermore this apparatus selected also muons of a given kinetic energy because the lead block let through only particle that had kinetic energy which was larger than the energy loss in the lead block. However, since the particles were required to stop in the chamber their kinetic energy as they exited the led block was very small. Hence, their initial energy was approximately equal to the energy loss in the lead block.

Using this apparatus the observed the track shown at the right of Fig. 17. This track had:

$$p = 0.3 \cdot B \cdot R = 0.3 \times 9.6 \times 10^4 \text{ Gauss} \cdot \text{cm} = 28.8 \text{ MeV}/c \quad (1)$$

and it had 6 times larger droplet density than an electron track of similar momentum. An electron at this momentum is already relativistic:

$$\beta\gamma = (28.8 \text{ MeV}/c)/0.511 \text{ MeV} = 56.4 \Rightarrow v_e \simeq c$$

Hence, the observed track ionized six times more than a relativistic electron which meant that:

$$\frac{\left(\frac{dE}{dx}\right)_{TRACK}}{\left(\frac{dE}{dx}\right)_{relativistic-e}} = \frac{1}{\beta_{TRACK}^2} = 6 \Rightarrow (\beta\gamma)_{TRACK} = 0.45 \quad (2)$$

From (1) and (2) they derived that the mass of this particle was:

$$m_{TRACK} = (28.8/0.45) \text{ MeV} \simeq 65 \text{ MeV}$$

So they had proved that the particle mass was indeed somewhere between the electron mass and the proton mass. These particles were what we call today muons, a heavier version of the electron, and have a well measured mass of  $m_\mu = 105.7 \text{ MeV}$ .



Evidently their experimental error was of the order of 100% although in their paper they claimed a 25% error. However, they did show beyond doubt the the new particle had a mass that was very different than either the proton, neutron or the electron masses and this was good enough to confirm the result of Anderson and Neddermeyer.

At the time this was an unexpected discovery and this is why I. I. Rabi (Nobel Price, Columbia University) asked “who ordered this?”. The muon did not seem to serve any purpose at the time. Even worse, physicists confused this with the pion (due to its similar mass) and thought that the muon (which they called mesotron at the time) was the Yukawa particle<sup>6</sup>. This sent them to the wrong path for a decade.

Today we know that the muon belongs to a category of particles which are called **leptons** and has the same properties as the electron but is approximately two hundred times heavier. Leptons are spin  $\frac{1}{2}$  fermions and come in three families. Each family has a charged particle and its electrically neutral neutrino partner (electron/electron-neutrino, muon/muon-neutrino, tau/tau-neutrino). The mass of the charged leptons is rising with the family. It is known today that neutrinos do have mass. However, their mass pattern is subject to intense investigations today.



**Figure 19:** Anderson(left) who discovered of the positron and the muon. Blackett (right) who pioneered the triggering techniques for cloud chambers.

<sup>6</sup> The last exercise in Homework Assignment 3 refers precisely to this issue.